# Optimal Two-Impulse Rendezvous Using Multiple-Revolution Lambert Solutions

Haijun Shen* and Panagiotis Tsiotras[†]

*Georgia Institute of Technology, Atlanta, Georgia 30332-0150*

The minimum-$\Delta V$, fixed-time, two-impulse rendezvous between two spacecraft orbiting along two coplanar unidirectional circular orbits (moving-target rendezvous) is studied. To reach this goal, the minimum-$\Delta V$, fixed-time, two-impulse transfer problem between two fixed points on two circular orbits is first solved. This fixed-endpoint transfer is related to the moving-target rendezvous problem by a simple transformation. The fixed-endpoint transfer problem is solved using the solution to the multiple-revolution Lambert problem. A solution procedure is proposed based on the study of an auxiliary transfer problem. When this procedure is used, the minimum $\Delta V$ of the moving-target rendezvous problem without initial and terminal coasting periods is obtained for a range of separation angles and times of flight. Thus, a contour plot of the cost vs separation angle and transfer time is obtained. This contour plot, along with a sliding rule, facilitates the task of finding the optimal initial and terminal coasting periods and, hence, obtaining the globally optimal solution for the moving-target rendezvous problem. Numerical examples demonstrate the application of the methodology to multiple rendezvous of satellite constellations on circular orbits.

## Introduction

**I**N this paper, we are interested in finding the best two-impulse solutions for a class of rendezvous problems. Specifically, we study the fixed-time, two-impulse rendezvous problem between two spacecraft. Both the chaser and the target spacecraft move on two coplanar circular orbits in the same direction. The motivation for investigating such two-impulse fixed-time rendezvous problems stems from our interest in solving multiple rendezvous problems between several vehicles in a satellite constellation. Clusters of satellites and satellite constellations (including formation flying schemes) promise to provide increased flexibility, autonomy, reliability, and operability compared to traditional single-spacecraft approaches.[1-3] In many cases, the satellites in the constellation can be serviced either from a vehicle launched from Earth for that purpose or by other satellites in the same constellation.[4] Such scenarios require a complete understanding of multiple orbital transfers between a number of satellites.

Before being able to solve the multiple-rendezvous problem for a satellite constellation (which may include dozens or hundreds of satellites) it is imperative to have a complete characterization for the simplest case of an optimal rendezvous, namely, between two satellites in a circular orbit. As a matter of fact, as shown in this paper, even the simple case of prioritizing the rendezvous maneuvers between three satellites is not clear from the outset. The results of this paper, thus, lay the foundation for solving efficiently optimal and suboptimal rendezvous strategies in a constellation with many satellites.

In Ref. 5 a solution procedure is outlined for the multiple-revolution Lambert problem. It is shown that given two points and a specified time of flight long enough to allow $N_{\max}$ revolutions for the chaser, there exist $2N_{\max} + 1$ Keplerian orbits that pass through the given two points. With the use of the solutions to the multiple-revolution Lambert problem, Prussing[5] studied the minimum-cost, fixed-time transfer between two fixed points on coplanar circular

orbits. He showed that allowing more than one revolution may reduce fuel consumption. However, Prussing does not identify which of the possible $2N_{\max} + 1$ solutions provides the least cost. As a result, the minimum-cost solution is obtained only after calculating all $2N_{\max} + 1$ candidates. In this paper, we provide an algorithm that quickly and efficiently identifies the optimal (minimum-$\Delta V$) solution without the need to calculate all $2N_{\max} + 1$ transfer orbits.

This paper is organized in the following manner: After the Introduction, the formulation of the minimum-$\Delta V$, fixed-time, fixed-endpoint orbital transfer problem is presented, then the auxiliary transfer problem is introduced and its solution is analyzed. The solution to the auxiliary transfer problem is then applied to the fixed-endpoint transfer problem. Next, solutions to the moving-target rendezvous problem without initial and final coasting periods are obtained for a range of separation angles and times of flight. The global optimal solution for the moving-target rendezvous problem can then be obtained by applying a sliding rule.[6] As an application to the proposed methodology, in the last section of the paper we analyze rendezvous maneuvers motivated by the problem of servicing satellites in a circular constellation.

## Fixed-Time, Fixed-Endpoint Transfer Between Circular Orbits

Given two points $P_1$ and $P_2$ in space, there are two elliptic orbits with the same semimajor axes that connect the two points, as shown in Fig. 1. In Fig. 1, $F$ and $F^*$ are the primary and secondary foci of the transfer orbits, $r_1$ and $r_2$ are the radii from $F$ to the points $P_1$ and $P_2$, respectively, $d$ is the length of the chord connecting $P_1$ and $P_2$, and $\theta$ is the central angle between $r_1$ and $r_2$. The two orbits in Fig. 1 belong to two separate categories: the long-path transfer orbits and short-path transfer orbits. As seen in Fig. 1, for a long-path transfer orbit, $F$ and $F^*$ lie on opposite sides of the $P_1 P_2$ line segment, whereas for a short-path transfer orbit, $F$ and $F^*$ lie on the same side of the $P_1 P_2$ line segment. For a given transfer time $t_f$, an $N$-revolution transfer orbit is an elliptic orbit passing through $P_1$ and $P_2$, and the time of travel along the $P_1 P_2$ arc plus $N$ complete revolutions is $t_f$. An $N$-revolution transfer then is one where the chaser spacecraft moves along the elliptic transfer orbit for $N$ complete revolutions plus the $P_1 P_2$ arc before meeting the target at $P_2$. In general, there is more than one elliptic orbit that passes through $P_1$ and $P_2$ for a given travel time $t_f$, depending on the number of revolutions allowed. These orbits are either long-path or short-path orbits with different semimajor axes.

According to Lambert (see Ref. 7), the time of flight is a function only of the semimajor axis $a$, the sum of the radii $r_1 + r_2$, and the
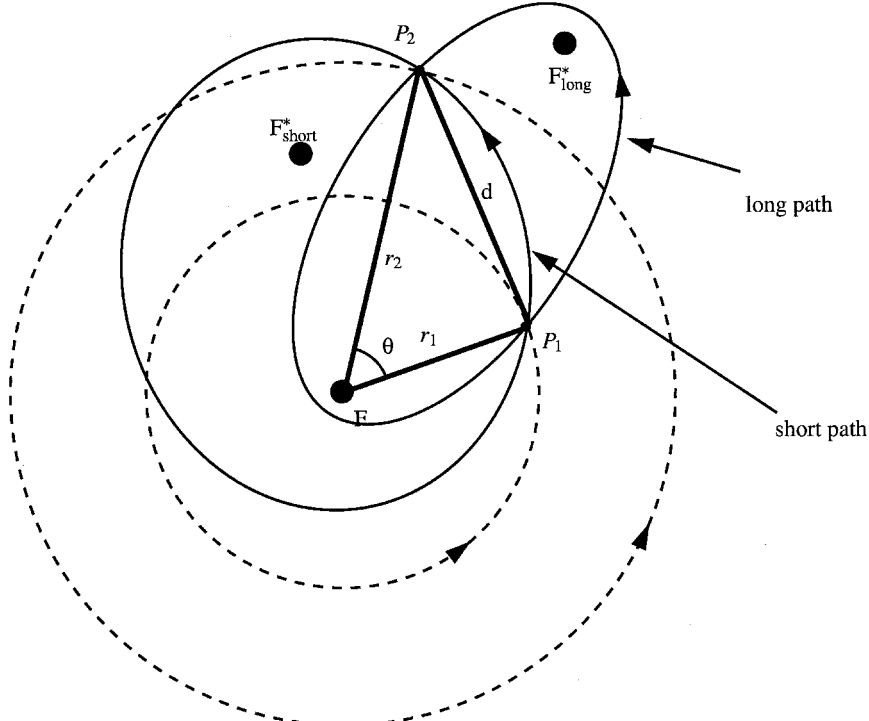
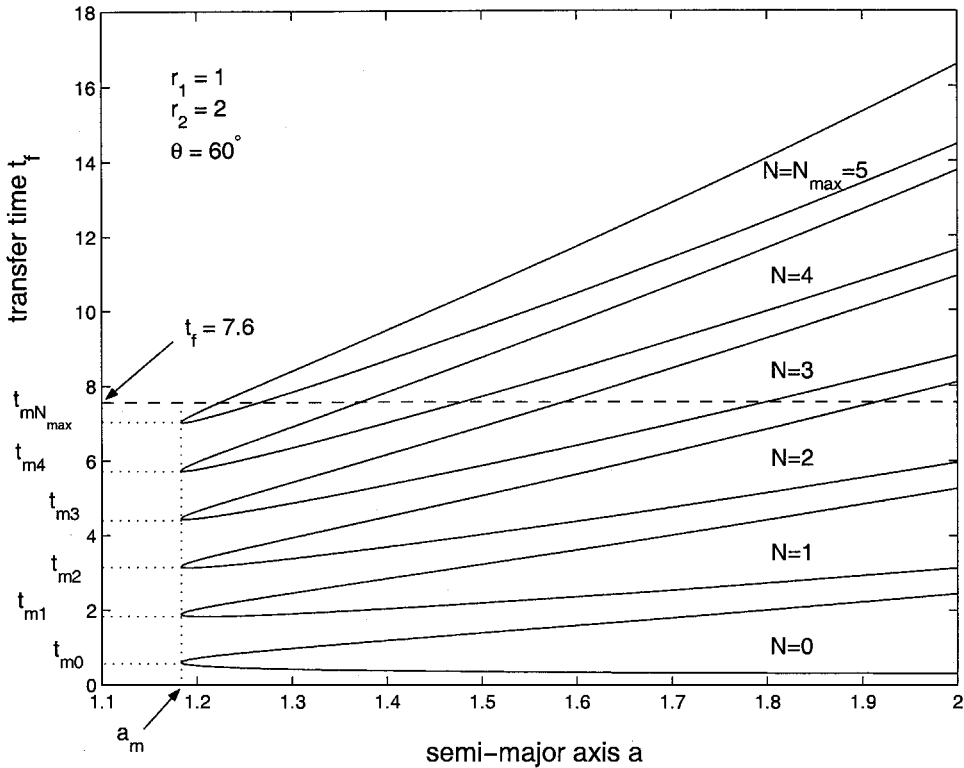**Fig. 1   Orbital geometry for Lambert problem.**



**Fig. 2   Example graph of $t_f$ vs $a$.**

chord length $d$. Lagrange's formulation of the Lambert problem can be generalized to the multiple-revolution case as[5]

$$\sqrt{\mu} t_f = a^{\frac{3}{2}} [2N\pi + \alpha - \beta - (\sin\alpha - \sin\beta)] \qquad (1)$$

where $\mu$ is the gravitational parameter, $N$ is the number of allowed revolutions, and $\alpha$ and $\beta$ are defined as follows:

$$\sin(\alpha/2) = [s/(2a)]^{\frac{1}{2}}, \qquad \sin(\beta/2) = [(s-d)/(2a)]^{\frac{1}{2}} \quad (2)$$

where $s = (r_1 + r_2 + d)/2$. A geometric interpretation of the variables $\alpha$ and $\beta$ can be found in Ref. 8.

In the following, canonical units are used in the calculations. That is, the reference circular orbit has radius $r_1 = 1$ and period 1. Hence, $\mu = 4\pi^2$, and the velocity unit is the reference orbital speed divided by $2\pi$.

An example plot of $t_f$ vs the semimajor axis $a$ is shown in Fig. 2. Figure 2 is drawn with the help of Eq. (1). $N$ denotes the number of revolutions. The plot in Fig. 2 corresponds to the case where $r_1 = 1$, $r_2 = 2$, and $\theta = 60$ deg. For each $N$, two solution branches exist, an upper branch and a lower branch. The upper branch corresponds to a long path for $\theta \leq 180$ deg, and a short path for $\theta \geq 180$ deg; the lower branch corresponds to a short path for $\theta \leq 180$ deg, and a

long path for $\theta \geq 180$ deg. For each $N \geq 1$, there are two semimajor axes corresponding to the same $t_f$, and they define two $N$-revolution transfer orbits (short-path and long-path orbits). However, for $N = 0$, the lower branch is monotonically decreasing and so there is only one semimajor axis that corresponds to the same $t_f$ (either for the short-path orbit or for the long-path orbit). Therefore, for a given $t_f$, there are $2N_{\max} + 1$ solutions for the multirevolution Lambert problem, where $N_{\max}$ is the maximum number of allowed revolutions. For example, in Fig. 2, it is shown that for a time of flight of $t_f = 7.6$ we have $N_{\max} = 5$. It is clear that there is a total of 11 semimajor axes that determine 11 different transfer orbits connecting $P_1$ and $P_2$.

A minimum-energy Keplerian orbit always exists connecting two given fixed points in space.[7] The semimajor axis of this minimum energy orbit is given by $a_m = s/2$. This is the minimum semimajor axis shown in Fig. 2. (This is the same for all branches.) The travel time corresponding to an $N$-revolution transfer orbit with semimajor axis $a_m$ is denoted by $t_{m\ell}$, $\ell = 0, 1, \ldots, N_{\max}$. A procedure for determining $N_{\max}$ and solving for all $2N_{\max} + 1$ transfer orbits for a given $t_f$ is provided in Ref. 5.

Next, we consider the case where the two endpoints $P_1$ and $P_2$ lie on two coplanar unidirectional circular orbits. The objective is to find the minimum-$\Delta V$ transfer orbit for a chaser at $P_1$ to rendezvous with a target at $P_2$ in a given time of flight $t_f$. Both the chaser and the target are moving along the two circular orbits before the rendezvous maneuver, and $P_2$ is the location where the rendezvous takes place. This scenario is also shown in Fig. 1. For ease of reference we henceforth refer to this problem as the fixed-time, fixed-endpoint transfer problem. In the following, "cost" and $\Delta V$ will be used interchangeably. Prussing[5] has listed and compared the minimum costs for various cases of ratios of orbital radii and central angles. He is interested in the question of whether the long-path or the short-path transfer orbit renders the minimum cost. He also studies the optimal number of revolutions corresponding to the minimum-cost solution. In Ref. 5, it is shown that there are no clear patterns to facilitate the answer to these two questions. Therefore, a minimum-cost transfer orbit is determined after all of the $2N_{\max} + 1$ solutions have been calculated and compared.

In the following sections, an auxiliary orbital transfer problem is introduced. This problem is slightly different from the formulation of the original fixed-time, fixed-endpoint transfer problem in the sense that the transfer time in the auxiliary transfer problem is free. It will be shown in the sequel that the solution to this auxiliary transfer problem greatly facilitates the solution to the underlying fixed-time, fixed-endpoint transfer problem. Indeed, at most two (instead of all $2N_{\max} + 1$) solutions need to be computed to yield the minimum cost.

## Auxiliary Transfer Problem

The auxiliary transfer problem also seeks the two-impulse, minimum-cost transfer between any two points $P_1$ and $P_2$ in two coplanar circular orbits. However, unlike the fixed-time, fixed-endpoint transfer problem, in the auxiliary transfer problem, the time of flight is free. The main purpose of the auxiliary transfer problem is to study the relation between $\Delta V$ and the semimajor axis. An explicit expression of the $\Delta V$ needed to transfer from $P_1$ to $P_2$ along a Keplerian orbit can be obtained from classical orbital mechanics, as follows[9]:

$$\Delta V = \Delta V_1 + \Delta V_2 \qquad (3)$$

where $\Delta V_1$ and $\Delta V_2$ are the costs incurred at points $P_1$ and $P_2$. They are given by

$$\Delta V_i = \sqrt{v_i^2 + v_{ic}^2 - 2v_i v_{ic} \cos\phi_i}, \qquad i = 1, 2 \qquad (4)$$

where $v_1$ and $v_2$ are the orbital speeds at points $P_1$ and $P_2$ on the transfer orbit, $v_{1c}$ and $v_{2c}$ are the orbital speeds on the two circular orbits, and $\phi_1$ and $\phi_2$ are the elevation angles, that is, the angles at $P_1$ and $P_2$ between the velocities on the circular orbits and the velocities on the transfer orbit.

Note that allowing for multiple revolutions does not change the $\Delta V$. However, the more the number of revolutions the longer

the transfer time will be. As a result, as shown in Fig. 2, there are two transfer orbits passing through $P_1$ and $P_2$ that have the same semimajor axis. One is the long-path transfer orbit, and the other the short-path transfer orbit. These two transfer orbits correspond to different times of travel. It is shown in the Appendix that the cost $\Delta V$ for both the long-path and the short-path solutions of the auxiliary orbital transfer problem are a function of only the semimajor axis of the transfer orbit. However, the analytical relationship between $a$ and $\Delta V$ is rather complicated. Nevertheless, numerical results suggest a great deal of insight.

To this end, we have plotted in Fig. 3 the relationship of $\Delta V$ vs $a$ for the cases where $r_1 = r_2$ and $r_2 = 2r_1$. In both cases $\theta = 120$ deg. Extensive numerical studies show that the plots of $\Delta V$ vs $a$ for other combinations of $r_1$, $r_2$, and $\theta$ have similar characteristics as in Fig. 3. Thus, Fig. 3 will be used to induce salient properties of the solution. From Fig. 3, it is evident that there is a unique semimajor axis that corresponds to the minimum $\Delta V$. Let this be denoted by $a_{\min}$. The elliptic Keplerian transfer orbit with semimajor axis $a_{\min}$ is the solution to the auxiliary transfer problem. Interestingly, this transfer orbit is always a short-path transfer orbit. For the case where $r_1 = r_2$, we have that $a_{\min} = r_1 = r_2$, and, hence, the total $\Delta V = 0$. Figure 3 shows that $a_{\min}$ is not a stationary point for $\Delta V$. This can also be verified that $d(\Delta V)/da$ does not exist at $a_{\min} = r_1 = r_2$ because in this case the eccentricity is zero. However, for the case $r_1 \neq r_2$, Fig. 3 shows that $a_{\min}$ is a stationary point for $\Delta V$. Hence, $a_{\min}$ can be calculated by setting $d(\Delta V)/da = 0$. Numerical schemes such as the Newton–Raphson algorithm or the bisection method can be used to compute $a_{\min}$. Detailed expressions for $\Delta V$ and $d(\Delta V)/da$ can be found in the Appendix.

As shown in Fig. 3, for a given semimajor axis, following the long-path transfer orbit always costs more than following the short-path transfer orbit. The cost associated with a long-path transfer orbit is monotonically increasing with $a$. For a short-path transfer orbit, however, the cost increases if the semimajor axis $a$ is greater than $a_{\min}$ and decreases if the semimajor axis $a$ is less than $a_{\min}$. Caution has to be exercised because it is not true that any long-path orbit always results in a larger cost than any short-path orbit. For example, as seen in Fig. 3, a short-path transfer orbit with a large semimajor axis could be more costly than a long-path transfer orbit with a smaller semimajor axis.

## Solution to the Fixed-Time, Fixed-Endpoint Transfer Problem

Based on the observations made earlier about the characteristics of $\Delta V$ with respect to $a$ for the auxiliary transfer problem, the computations required for the minimum-$\Delta V$ solution for a fixed-time, fixed-endpoint transfer problem can be significantly reduced. This is especially true for cases with large times of travel that allow a large number of revolutions. As a result, in some cases, the minimum-$\Delta V$ solution is readily chosen by inspection; in other cases, only two of the $2N_{\max} + 1$ solutions need to be calculated and compared to obtain the minimum-$\Delta V$ transfer orbit.

Recall that given a fixed-time, fixed-endpoint transfer problem with transfer time $t_f$, there are $2N_{\max} + 1$ solution candidates, that is, there are $2N_{\max} + 1$ semimajor axes corresponding to the same time of flight on the plot of $t_f$ vs $a$ (Fig. 2). Each of these $2N_{\max} + 1$ semimajor axes corresponds to an elliptic Keplerian transfer orbit. The semimajor axis that corresponds to the minimum-$\Delta V$ transfer orbit can be chosen by applying the observations made earlier about the auxiliary transfer problem to these $2N_{\max} + 1$ semimajor axes. In the following, we present a solution procedure to achieve this goal. This will be demonstrated on the plot of $t_f$ vs $a$ for a case $\theta \leq 180$ deg. The case when $\theta > 180$ deg can be treated similarly and is discussed briefly at the end of this section.

We need to calculate the times of transfer $t_{N\ell}$ and $t_{Ns}$ from $P_1$ to $P_2$ along the long-path and short-path transfer orbits with semimajor axis $a_{\min}$ with $N$ revolutions, where $N = 0, 1, \ldots, N_{\max}$. This calculation can be done in a straightforward manner using Eq. (1). In the sequel, the subscript $\ell$ stands for the long-path and the subscript $s$ stands for the short-path transfer orbit. Figure 4 shows, for instance, the values of $t_{Ns}$ and $t_{N\ell}$ for $N = 4$.
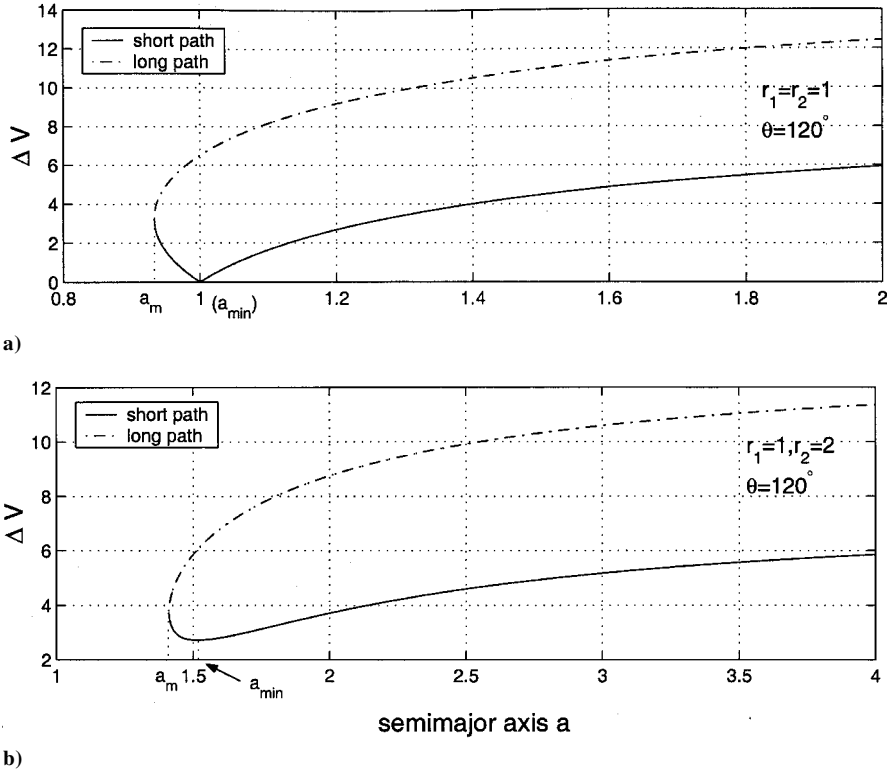
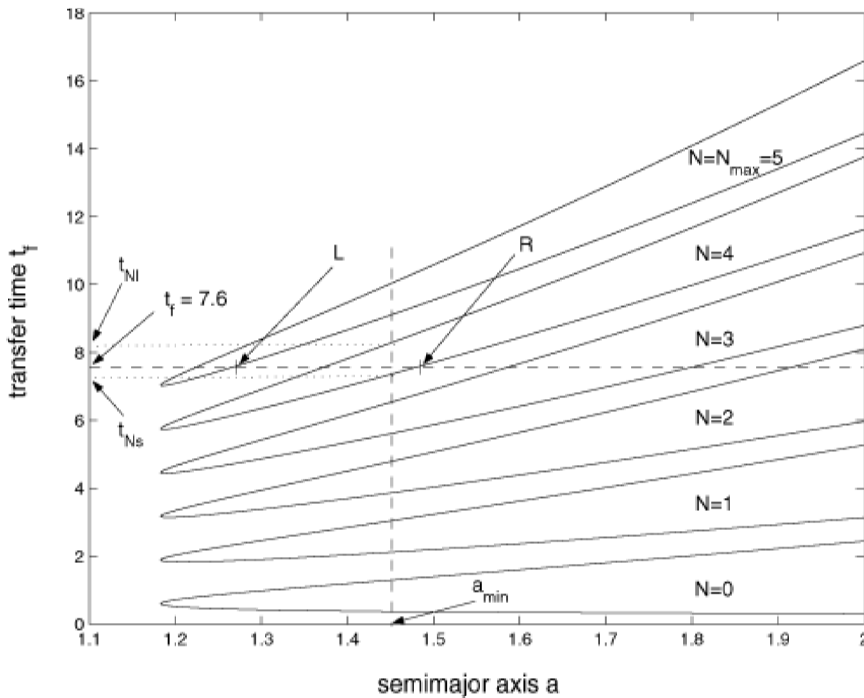Fig. 3   $\Delta V$ vs $a$: a) $r_1 = r_2$ and b) $r_1 \neq r_2$.



Fig. 4   Case 2, $t_{Ns} \leq t_f \leq t_{N\ell}$ and $N \neq N_{max}$.

According to the comparison between $t_f$ and $t_{N\ell}$ and $t_{Ns}$, $(N = 0, 1, \ldots, N_{max})$, there are four cases to consider.

1) If $N_{max} = 0$, no revolution is allowed (case 1). Clearly, there is only one solution candidate, which is either a long-path or a short-path solution. Thus, this is the optimal solution.

For cases 2, 3, and 4, we assume that $N_{max} \geq 1$.

2) If $t_{Ns} \leq t_f \leq t_{N\ell}$ and $N \neq N_{max}$, then $a_{min}$ is between the semi-major axes of the long-path transfer orbit and the short-path transfer orbit with $N < N_{max}$ revolutions (case 2). This is shown in Fig. 4. Recall that any short-path transfer orbit with $a \leq a_{min}$ costs less

than any long-path transfer orbit. Thus, the optimal solution is a short-path transfer orbit. In addition, for short-path transfer orbits, $\Delta V$ monotonically decreases for $a \leq a_{min}$ and monotonically increases for $a \geq a_{min}$. Therefore, either the short-path $N$-revolution orbit (point $R$ in Fig. 4) or the short path $(N + 1)$-revolution orbit (point $L$ in Fig. 4) provides the minimum cost. However, there is no a priori knowledge regarding whether the former or the latter is the minimum-cost solution. Thus, both transfer orbits corresponding to points $R$ and $L$ in Fig. 4 need to be calculated. The one with the smaller cost is the optimal transfer orbit. A special subcase occurs
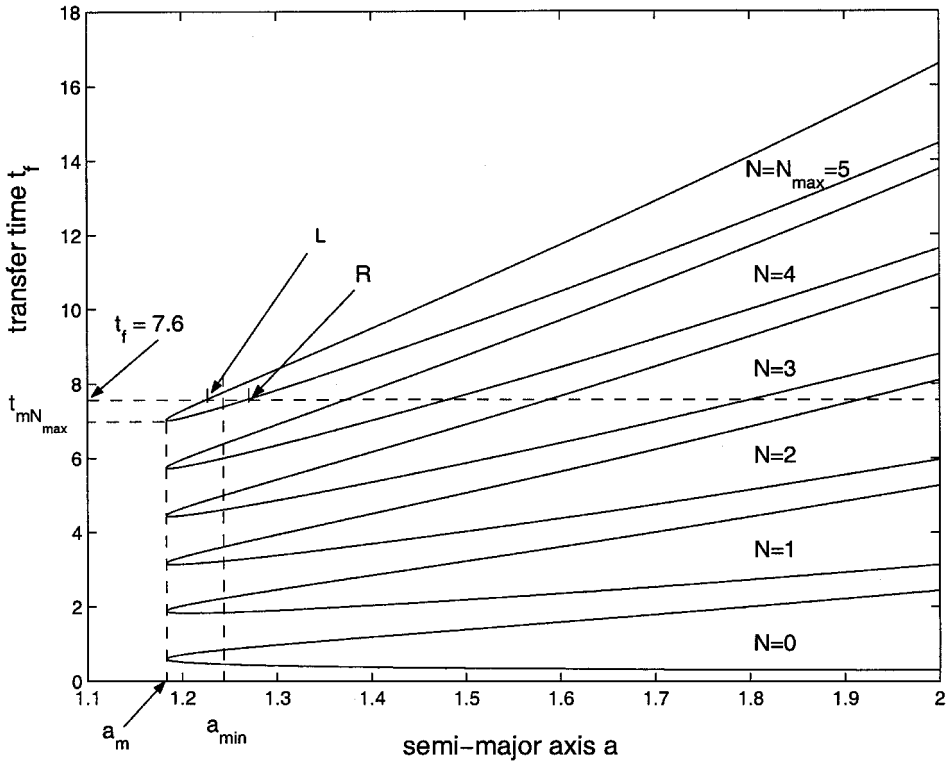
**Fig. 5** Subcase 3a, $t_{N_{\max}s} \leq t_f \leq t_{N_{\max}\ell}$ and $t_f \geq t_{mN_{\max}}$.
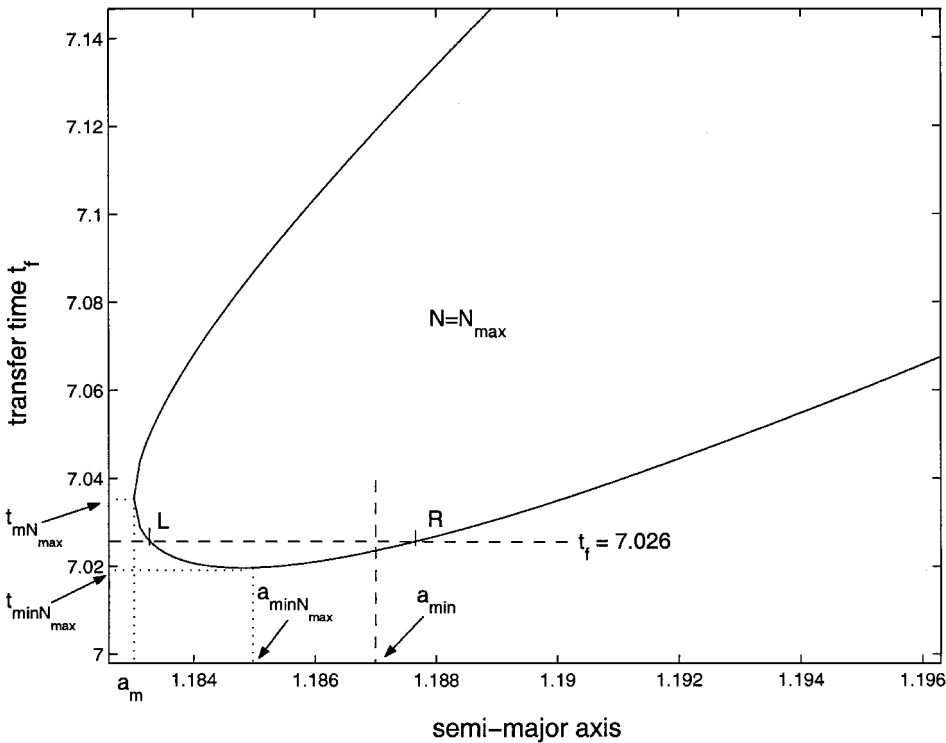


**Fig. 6** Subcase 3b, $t_{N_{\max}s} \leq t_f \leq t_{N_{\max}\ell}$ and $t_{\min N_{\max}} \leq t_f \leq t_{mN_{\max}}$.

when $N = 0$. In this case, the short-path one-revolution orbit with $a < a_{\min}$ provides the minimum cost because there is no short-path solution for $a \geq a_{\min}$.

3) Case 3, when $t_{Ns} \leq t_f \leq t_{N\ell}$ and $N = N_{\max}$, is complicated by the fact that the short-path branch for $N \geq 1$ is not monotonically increasing. Instead, $t_f$ has a stationary point. Let us denote by $t_{\min N}$ the value of the time of travel at this stationary point and by $a_{\min N}$ the corresponding semimajor axis. There are two subcases to consider.

a) Case 3a, when $t_f \geq t_{mN_{\max}}$, is shown in Fig. 5. Following a similar argument as in case 2, only two solutions need to be

calculated. These are the long-path and the short-path orbits corresponding to $N = N_{\max}$ (points $L$ and $R$ in Fig. 5). The smaller of the two renders the minimum-cost transfer orbit.

b) Figure 6 shows case 3b, when $t_{\min N_{\max}} \leq t_f \leq t_{mN_{\max}}$. The two short-path $N_{\max}$-revolution solutions (points $L$ and $R$ in Fig. 6) need to be calculated and compared. The smaller one renders the minimum-cost transfer orbit.

4) In case 4, $t_{N\ell} \leq t_f \leq t_{(N+1)s}$, that is, $a_{\min}$ is between the semimajor axis of the $N$-revolution long-path transfer orbit and the semimajor axis of the $(N + 1)$-revolution short-path transfer orbit. There are three subcases to consider.
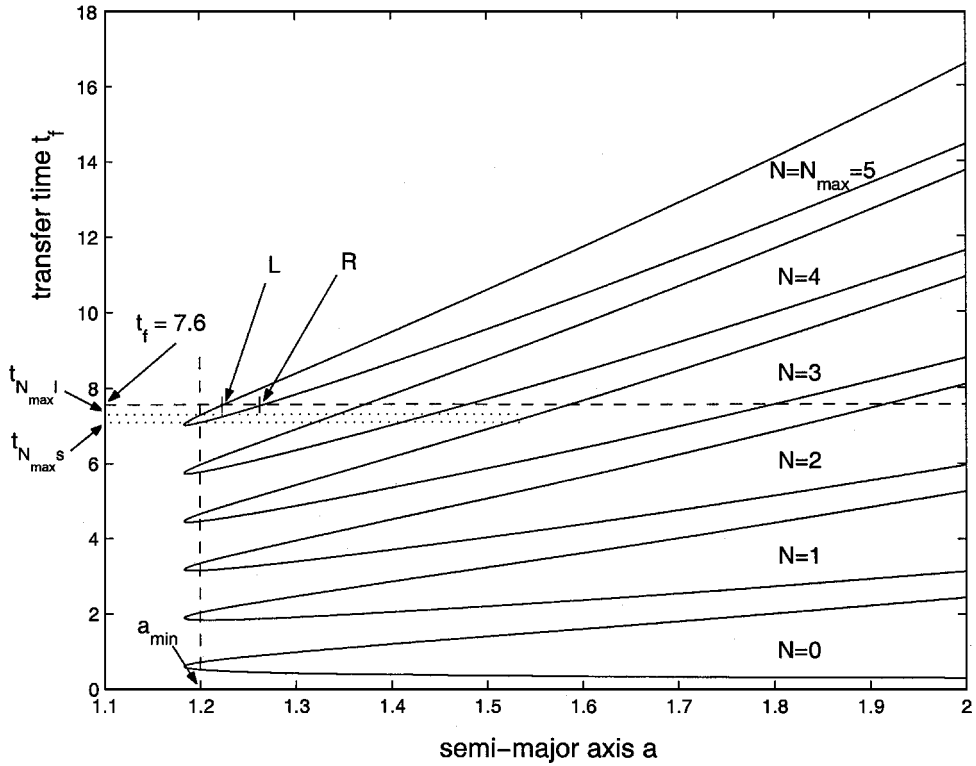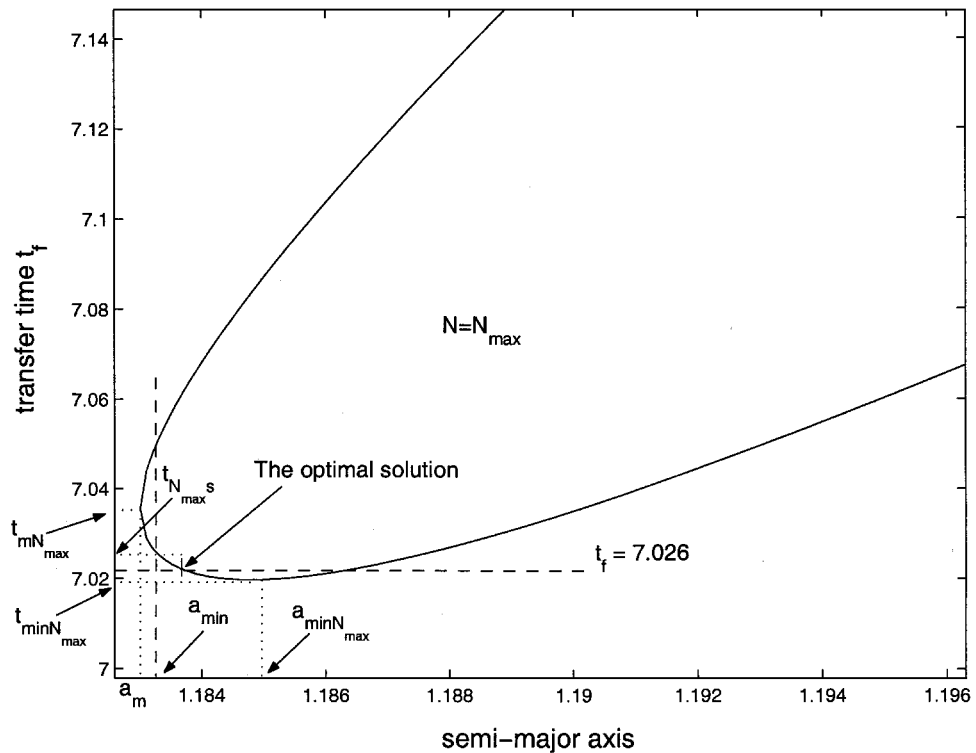
**Fig. 7** Case 4a, $t_f \geq t_{N_{\max}\ell}$.



**Fig. 8** Case 4b, $t_{(N_{\max}-1)\ell} \leq t_f \leq t_{N_{\max}s}$ and $a_m \leq a_{\min} \leq a_{\min N_{\max}}$.

a) In subcase 4a, $t_f \geq t_{N_{\max}\ell}$, that is, $a_{\min}$ is less than the least semimajor axis candidate, as seen in Fig. 7. In this case, only two candidates need to be calculated (points $L$ and $R$ in Fig. 7). These are the $N_{\max}$-revolution long- and short-path transfer orbits. The one with the smaller $\Delta V$ is the optimal solution.

b) In subcase 4b, $t_{(N_{\max}-1)\ell} \leq t_f \leq t_{N_{\max}s}$ but $a_m \leq a_{\min} \leq a_{\min N_{\max}}$. This is shown in Fig. 8. In this case, $a_{\min}$ is less than the least semimajor axis candidate. Because the closest semimajor

axis candidate corresponds to a short-path transfer orbit, it follows that this transfer orbit is the minimum-$\Delta V$ solution.

c) Subcase 4c includes all remaining cases under the condition of case 4. The situation is shown in Fig. 9. The $(N+1)$-revolution short-path transfer orbit requires less $\Delta V$ than any other solution with $a \leq a_{\min}$ and any long-path transfer orbit. Similarly, the $N$-revolution short-path transfer orbit requires less $\Delta V$ than any other short-path transfer orbit with $a \geq a_{\min}$. Therefore, as before,
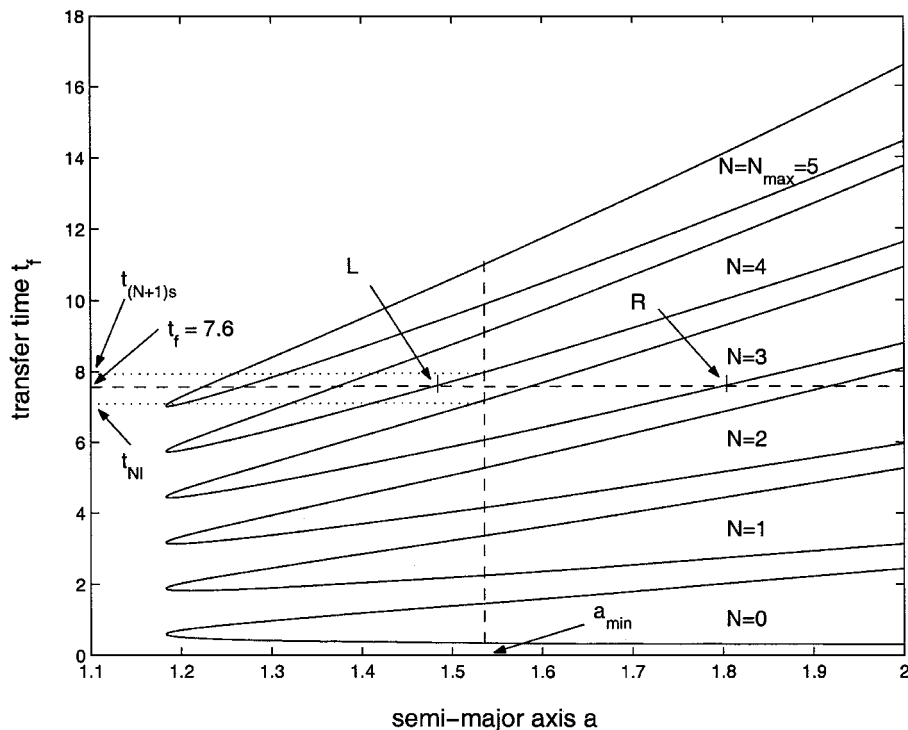
**Fig. 9    Case 4c, $t_{N\ell} \leq t_f \leq t_{(N+1)s}$, excluding subcases 4a and 4b.**

only two solutions need to be calculated and compared. These are the $N$-revolution and $N+1$ revolution short-path solutions (points $L$ and $R$ in Fig. 9). The one with the smaller $\Delta V$ represents the minimum-$\Delta V$ transfer orbit. If $N = 0$, the one-revolution short-path transfer orbit provides the minimum $\Delta V$.

The described procedure allows one to determine the minimum-$\Delta V$ transfer orbits for fixed-time, fixed-endpoint transfer problems where $\theta \leq 180$ deg. However, similar rules can be obtained for cases where $\theta > 180$ deg. In such cases, the lower branch corresponds to a long-path transfer orbit and the upper branch corresponds to a short-path transfer orbit. For brevity, we do not elaborate any further on the case $\theta > 180$ deg; the interested reader should be able to derive the corresponding results vis-à-vis the case $\theta \leq 180$ deg.

## Minimum-$\Delta V$, Fixed-Time, Two-Impulse Rendezvous Between Circular Orbits

### Problem Description

So far we have presented a procedure for obtaining the fixed-time, minimum-$\Delta V$ transfer orbit between two fixed points on two coplanar unidirectional circular orbits. In this section, we apply this procedure to find solutions to the moving-target rendezvous problem. To this end, consider two space vehicles (denoted by $s_1$ and $s_2$) in two coplanar circular orbits moving in the same direction. Vehicle $s_1$ is in the lower orbit, and $s_2$ is in the higher orbit. The initial separation angle $\theta_0$ from $s_1$ to $s_2$ is given. The objective is to find the minimum-$\Delta V$, two-impulse trajectory for $s_1$ to rendezvous with $s_2$ in a given time $t_f$. Although $s_2$ initially leads $s_1$ by the angle $\theta_0$, the central angle measured from $s_1$ to the location where the rendezvous is supposed to take place is

$$\theta = \theta_0 + t_f \omega_2 \qquad (5)$$

where $\omega_2$ is the orbital frequency of the outer orbit. This is because $s_2$ moves along the outer circular orbit during the maneuver. Essentially, once $\theta$ is known, that is, the projected rendezvous location is obtained, the moving-target rendezvous problem is transformed into a fixed-endpoint transfer problem between $s_1$ and the projected rendezvous location. Therefore, the aforementioned solution procedure can be applied to this problem as well.

### Contour Plots

For any two coplanar circular orbits, minimum-$\Delta V$ transfer orbits can be obtained for a range of initial separation angles and transfer times. Thus, a contour plot of the minimum $\Delta V$ can be obtained as a function of the separation angles and the transfer times. Figure 10 shows such a contour plot where $r_1 = r_2$, and Fig. 11 shows a contour where $r_1 = 1$ and $r_2 = 1.5$.

For the case $r_1 = r_2$ (Fig. 10), the absolute minimum cost (which is zero in this case) occurs along the vertical lines $\theta_0 = n \times 360$ deg, $n = 0, \pm 1, \pm 2, \ldots$. There are isolated nonzero local stationary points, which appear in a saddle pattern. Some rather abrupt changes of the $\Delta V$ as $t_f$ or $\theta_0$ changes are observed at the points $t_f \approx n + 0.5$, $n = 1, 2, \ldots$, and when $\theta_0$ is slightly larger than the integral multiples of 360 deg. These abrupt changes are mainly due to the steep jumps or drops of $\Delta V$ when the number of revolutions associated with the optimal solution changes with the total time of flight. When $r_2$ deviates from $r_1$, the characteristics of the contours change drastically, as shown in Fig. 11. There are no connected regions of absolute minima, but, instead, isolated local minima are observed resembling a central node pattern. These local minima are in fact global minima because they correspond to the cost of a Hohmann transfer. Note that the local minima when $t_f \geq 1.5$ correspond to multiple-revolution Hohmann transfers. Similarly to the case when $r_1 = r_2$, stationary points in a saddle pattern are also observed, as well as abrupt changes in the cost close to Hohmann transfers for $t_f \geq 1.5$.

### Initial and Final Coastings

Thus far, we have presented a procedure to obtain the solution for the moving-target rendezvous problem. Note that the solution does not involve any initial and final coasting periods. A coasting arc is defined as a trajectory during which gravity is the only external force, that is, there is no thrust. In many cases, it is advisable that the first impulse be applied some time after the starting time, and the second impulse be applied some time before the final time $t_f$. The waiting period after the starting time is called the initial coasting, and the time from the second impulse to the final time is called the final (or terminal) coasting. Clearly, during the initial coasting period, both the chaser and the target move along their respective orbits, whereas during the final coasting period, both the chaser and the target move together on the orbit of the latter.

From Eq. (5), it can be seen that allowing initial and/or final coasting changes the value of the central angle $\theta$ and the actual time of flight between the two impulses. Thus, initial and/or terminal
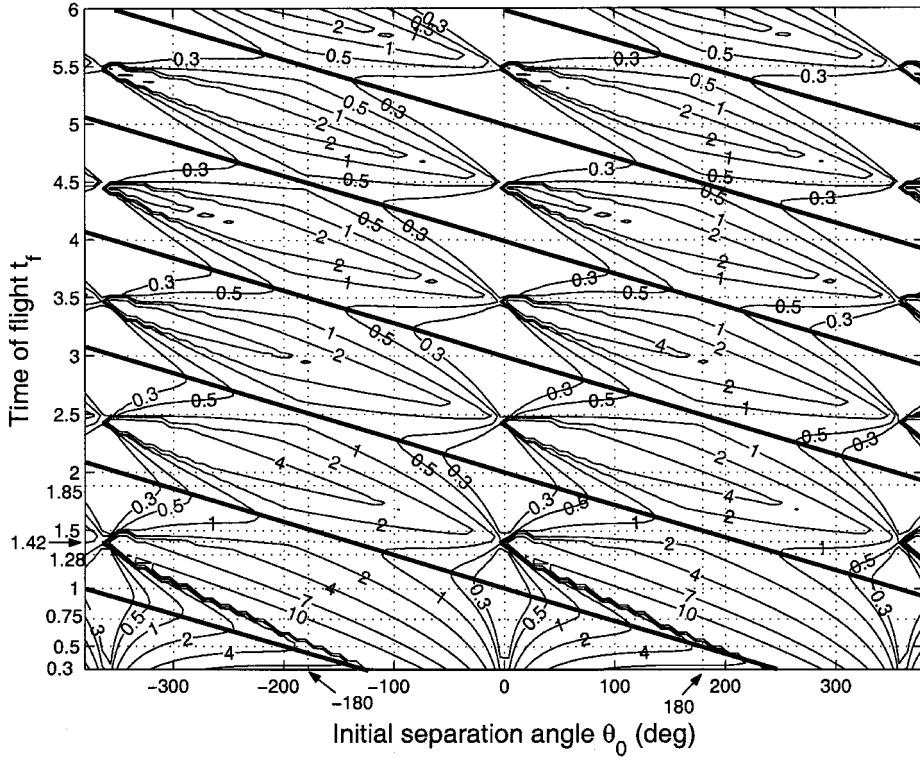
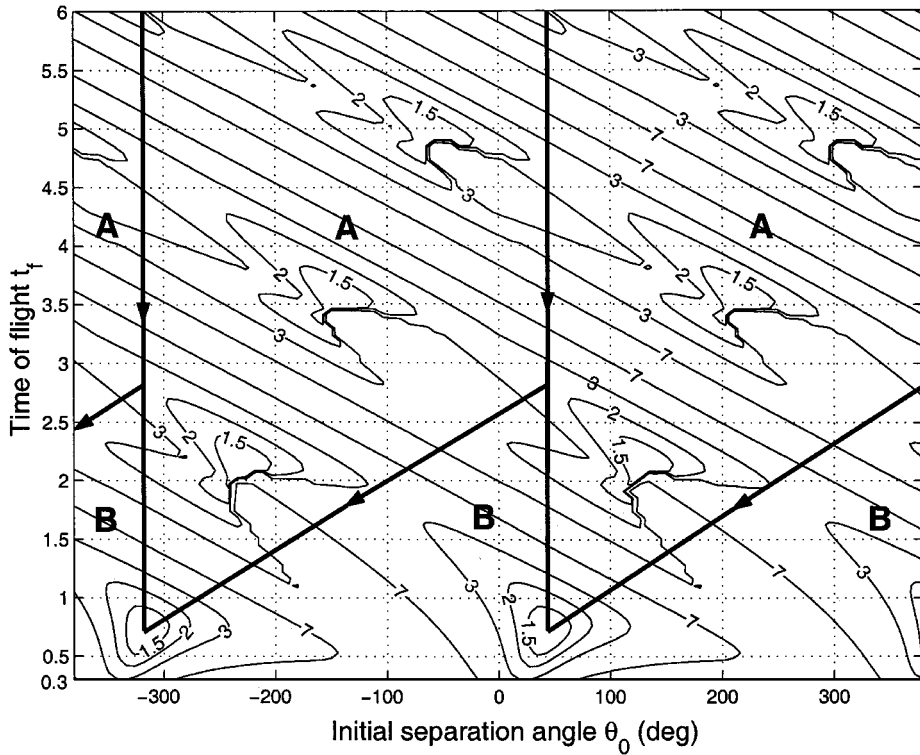Fig. 10   Contour of $\Delta V$ when $r_1 = r_2$.



Fig. 11   Contour of $\Delta V$ when $r_1 = 1$ and $r_2 = 1.5$.

coastings allow the two spacecraft to achieve a more favorable configuration. As a result, if initial and/or terminal coasting is allowed, it is possible to perform the desired moving-target rendezvous with a lower cost.

Suppose that we are given an initial separation angle $\theta_{00}$ and a total transfer time $t_{f0}$. Then after an initial coasting period $t_{c0}$, the separation angle $\theta_0$ becomes

$$\theta_0 = \theta_{00} - t_{0c}(\omega_1 - \omega_2) = \theta_{00} - (t_{f0} - t_{f1})(\omega_1 - \omega_2)$$

$$= (\omega_1 - \omega_2)t_{f1} + [\theta_{00} - t_{f0}(\omega_1 - \omega_2)] \qquad (6)$$

Hence,

$$t_{f1} = [1/(\omega_1 - \omega_2)]\theta_0 - [\theta_{00}/(\omega_1 - \omega_2) - t_{f0}] \qquad (7)$$

where $t_{f1}$ is the remaining transfer time after the initial coasting and $\omega_1$ is the orbital frequency of the inner orbit. Therefore, on the contour plot an initial coasting results in the point $(\theta_0, t_f)$ moving down along a straight line with slope of $1/(\omega_1 - \omega_2)$. On the other hand, a final coasting period $t_{fc}$ does not change the initial separation angle, but it shortens the time spent on the transfer orbit. Thus, a final coasting results in the point $(\theta_0, t_f)$ moving down along a vertical
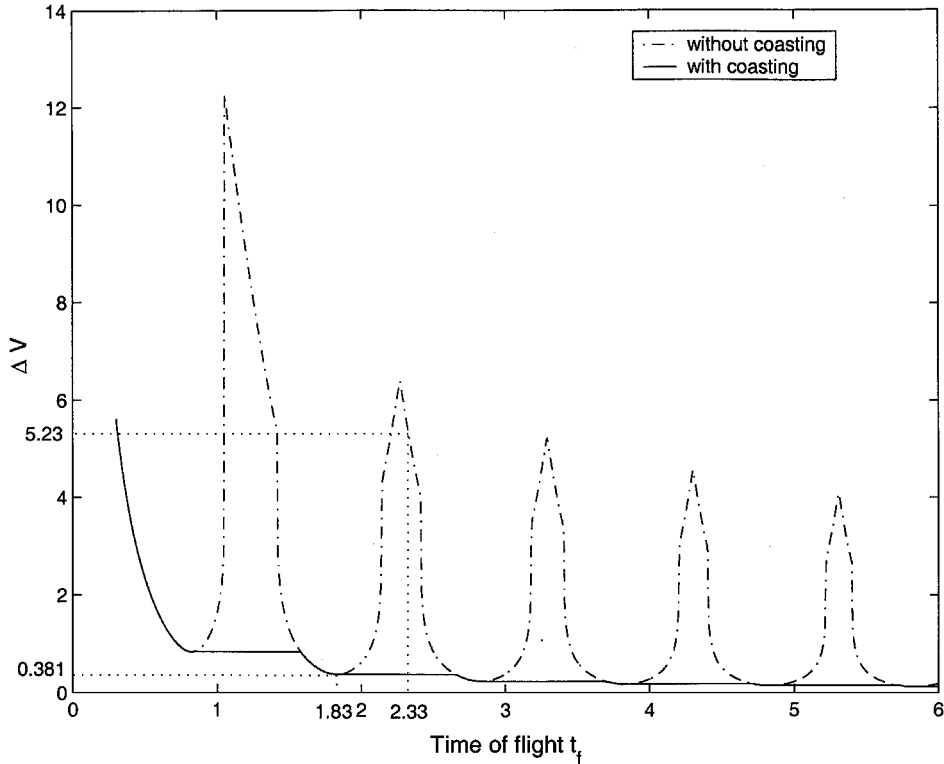
Fig. 12    $\Delta V$ vs $t_f$ when $r_1 = r_2$ and $\theta_0 = 60$ deg, with and without final coasting.

line while $\theta_0$ remains unchanged. The effect of an initial or a final coasting is shown in Fig. 11.

**The Sliding Rule**

With these contour plots and the knowledge of how the initial and terminal coastings affect the solutions, it is now straightforward to find the global minimum cost. Given an initial separation angle $\theta_0$ and a transfer time $t_f$, the initial and terminal coastings can be determined by a sliding rule. To make this point clear, let us first refer to Fig. 10 where $r_1 = r_2$. In this case, an initial coasting does not change the relative geometry of the two spacecraft, so that only the terminal coasting period needs to be determined. The given separation angle $\theta_0$ and the final time $t_f$ correspond to a single point on the contour plot. Any point with the same $\theta_0$ but with a transfer time $t_t \leq t_f$ also performs the required rendezvous with a terminal coasting of $t_{fc} = t_f - t_t$. The transfer time $t_t$ that yields the least $\Delta V$ can be easily picked from the contour plot. It is observed that, along a vertical line in Fig. 10 as $t_f$ increases, local minima and local maxima of $\Delta V$ appear alternately. This is shown by the dash-dotted curve in Fig. 12 for the special case when $\theta_0 = 60$ deg. Not surprisingly, the values of the local minima decrease as $t_f$ increases, and this trend persists for all $0 \leq \theta_0 \leq 360$ deg. Therefore, the optimal amount of terminal coasting can be picked as follows. Given $t_f$, we decrease $t_f$ while holding $\theta_0$ unchanged until the first local stationary minimum is encountered. Denote the corresponding time $t_t$. If $\Delta V(\theta_0, t_f) < \Delta V(\theta_0, t_t)$, then no terminal coasting can give a smaller $\Delta V$. However, if $\Delta V(\theta_0, t_f) \geq \Delta V(\theta_0, t_t)$, then the terminal coasting period is $t_f - t_t$. Figure 12 shows this scheme for computing the proper amount of terminal coasting for the case $\theta_0 = 60$ deg. The solid line represents the cost with proper terminal coasting. For example, as shown in Fig. 12, for a given time of flight of $t_f = 2.33$, the cost for the rendezvous maneuver without terminal coasting is 5.23. However, this rendezvous can be achieved by a transfer with time of flight $t_f = 1.83$ plus a terminal coasting of duration 0.5. The new cost is reduced to 0.381. The portions in Fig. 12 where the solid line and the dash-dotted lines overlap represent rendezvous scenarios for which no final coasting can reduce the $\Delta V$.

Another observation that dramatically expedites the calculation of the final coasting for the case when $r_1 = r_2$ can be made. As shown in Fig. 10, the set of all local minima can be represented by the slanted solid lines. The slope of each slanted line is $-1/360$ deg, and they

all pass through points where the separation angle is zero and the times of flight are integers. That is, the local minima correspond to scenarios where the rendezvous site is the starting location of the chaser. With this information, and given the separation angle $\theta_0$ and the time of flight $t_f$, the largest transfer time less than $t_f$ that corresponds to a local minimum is given by

$$t_t = n - (\theta_0/360) \tag{8}$$

where $n = \lfloor (t_f + \theta_0/360) \rfloor$ denotes the largest integer that is smaller than $t_f + \theta_0/360$. There is no terminal coasting if $\Delta V(t_f, \theta_0) \leq \Delta V(t_t, \theta_0)$. Otherwise, the terminal coasting time is given by $t_f - t_t$. This observation allows us to eliminate the reliance on the contour plot when finding the optimal rendezvous in the case when both the target and chaser are in the same circular orbit.

For the case when $r_1 \neq r_2$, we may refer to Fig. 11. The local minima in a center node pattern represent Hohmann transfers. The two solid vertical lines represent transfer problems that can be achieved by a Hohmann transfer by adding an appropriate amount of final coasting. The slanted lines represent transfer problems that can be achieved by a Hohmann transfer by adding an appropriate amount of initial coasting. The whole contour plot is thus divided into upper and lower portions, with the upper portion labeled A and the lower portion B. A moving-target rendezvous problem in portion A can be achieved by a Hohmann transfer, with a unique combination of initial and final coastings. On the other hand, portion B consists of problems that cannot be achieved by a Hohmann transfer. However, for some points in portion B, a better cost can be obtained with either an initial coasting or a final coasting. For all other points in portion B, no coasting can decrease the cost.

The points in portions A and B can be completely characterized. For a moving-target rendezvous problem with given $r_1$, $r_2$, $t_f$, and $\theta_0$, we can calculate the time of flight $t_h$, and the required initial separation angle $\theta_h$ that the target leads the chaser for the Hohmann transfer.[9] Both $\theta_0$ and $\theta_h$ are assumed to be between 0 and 360 deg. If $\theta_0 < \theta_h$, we replace $\theta_0$ by $360 + \theta_0$ deg. Then the initial coasting time for the two satellites to achieve the separation angle $\theta_h$ can be written as

$$t_{0c} = (\theta_0 - \theta_h)/(\omega_1 - \omega_2) \tag{9}$$

Thus, if $t_f - t_{0c} > t_h$, the underlying rendezvous problem belongs to portion A, and the rendezvous can be accomplished by a Hohmann

transfer with an initial coasting period $t_{0c}$ and a final coasting period $t_{fc} = t_f - t_{0c} - t_h$. Otherwise, the problem belongs to portion B. For problems in portion B, we have to rely on the contour plot to find the optimal duration of initial coasting and/or final coasting.

*Remark*: The concept of the sliding rule was first mentioned briefly by Lion and Handelsman,[6] where it was used to demonstrate the necessary conditions for initial and final coasting arcs derived by Lawden's primer vector theory. However, it has not been used in the literature to calculate the globally optimal solution for a moving-target rendezvous problem.

## Application Examples

In this section, we make some observations on fixed-time, moving-target rendezvous problems arising from servicing satellites in a circular constellation. We are mainly interested in a scenario where the $n$ satellites are distributed (perhaps nonuniformly) along a circular orbit, as shown in Fig. 13. In Fig. 13, five satellites are shown, which are labeled by $s_i$, $i = 1, \ldots, 5$. The separation angles between satellite $s_1$ and satellites $s_2$, $s_3$, $s_4$ and $s_5$ are $\theta_2$, $\theta_3$, $\theta_4$, and $\theta_5$, respectively.

### Rendezvous with Two Neighbor Satellites

The first question we want to answer is the following: Given a fixed total time $t_f$, find the best rendezvous option for satellite $s_1$, namely, rendezvous with satellite $s_2$, or rendezvous with satellite $s_4$. At first glance, one may think that the cost for both options is the same if the separation angles are the same, that is, if $|\theta_2| = |\theta_4|$. Indeed, this conjecture is supported by a linear analysis using the Clohessy–Wiltshire (C–W) equations.[10] To this end, let us consider the current circular orbit as the reference orbit with satellite $s_2$ being the origin of the associated Euler–Hill coordinate frame for the C–W equations. Let the $x$ axis point along the radial direction and the $y$ axis point along the velocity direction (Fig. 13). In this frame, the initial coordinates for the satellite $s_1$ are given by $(0, -\theta_2)$. When the state transition matrix[11] is used, the final states and the initial states are related as

$$\begin{bmatrix} 0 \\ 0 \\ \dot{x}_f^- \\ \dot{y}_f^- \end{bmatrix} =$$

$$\begin{bmatrix} 4 - 3\cos\tau & 0 & \sin\tau & 2(1 - \cos\tau) \\ 6(\sin\tau - \tau) & 1 & -2(1 - \cos\tau) & 4\sin\tau - 3\tau \\ 3\sin\tau & 0 & \cos\tau & 2\sin\tau \\ 6(\cos\tau - 1) & 0 & -2\sin\tau & 4\cos\tau - 3 \end{bmatrix} \begin{bmatrix} 0 \\ -\theta_2 \\ \dot{x}_0^+ \\ \dot{y}_0^+ \end{bmatrix} \quad (10)$$
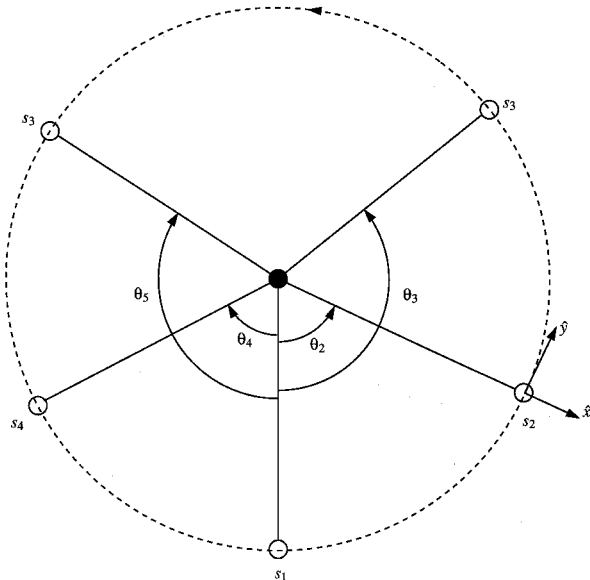


$\theta_5$    $\theta_3$    $\theta_4$    $\theta_2$    $\hat{y}$    $\hat{x}$

**Fig. 13   Satellite constellation on a circular orbit.**

where $(\dot{x}_0^+, \dot{y}_0^+)$ is the velocity vector of satellite $s_1$ immediately after it leaves its original location, $(\dot{x}_f^-, \dot{y}_f^-)$ is the velocity vector of $s_1$ immediately before it arrives at the satellite $s_2$, and $\tau$ is $2\pi$ times the transfer time. From the first two rows, of Eq. (10), obtains

$$\begin{bmatrix} 0 \\ 0 \end{bmatrix} = \begin{bmatrix} 0 \\ -\theta_2 \end{bmatrix} + \begin{bmatrix} \sin\tau & 2(1 - \cos\tau) \\ -2(1 - \cos\tau) & 4\sin\tau - 3\tau \end{bmatrix} \begin{bmatrix} \dot{x}_0^+ \\ \dot{y}_0^+ \end{bmatrix} \quad (11)$$

Equivalently,

$$\begin{bmatrix} \dot{x}_0^+ \\ \dot{y}_0^+ \end{bmatrix} = \frac{\theta_2}{8 - 3\tau\sin\tau - 8\cos\tau} \begin{bmatrix} -2(1 - \cos\tau) \\ \sin\tau \end{bmatrix} \quad (12)$$

From the last two rows of Eq. (10), we have

$$\begin{bmatrix} \dot{x}_f^- \\ \dot{y}_f^- \end{bmatrix} = \begin{bmatrix} \cos\tau & 2\sin\tau \\ -2\sin\tau & 4\cos\tau - 3 \end{bmatrix} \begin{bmatrix} \dot{x}_0^+ \\ \dot{y}_0^+ \end{bmatrix} \quad (13)$$

Substituting Eq. (12) into Eq. (13), it can be shown that

$$\begin{bmatrix} \dot{x}_f^- \\ \dot{y}_f^- \end{bmatrix} = \frac{\theta_2}{8 - 3\tau\sin\tau - 8\cos\tau} \begin{bmatrix} 2(1 - \cos\tau) \\ \sin\tau \end{bmatrix} = \begin{bmatrix} -\dot{x}_0^+ \\ \dot{y}_0^+ \end{bmatrix} \quad (14)$$

In the Euler–Hill coordinate frame, the velocity of $s_1$ immediately before the first impulse and the velocity of $s_2$ are both zero. Hence, $(\dot{x}_0^+, \dot{y}_0^+)$ and $(-\dot{x}_f^-, -\dot{y}_f^-)$ are the velocity changes (impulses) required for the rendezvous. Thus,

$$\Delta V_0 = \Delta V_f = \left\| \begin{bmatrix} \dot{x}_0^+ \\ \dot{y}_0^+ \end{bmatrix} \right\| = \frac{\sqrt{5 - 8\cos\tau + 3\cos^2\tau}}{|8 - 3\tau\sin\tau - 8\cos\tau|} |\theta_2| \quad (15)$$

The total cost $\Delta V_0 + \Delta V_f$ is proportional to the separation angle, which shows that the cost for the satellite $s_1$ to rendezvous with either $s_2$ or $s_4$ in a given time is the same, as long as $|\theta_2| = |\theta_4|$.

Contrary to our intuition and the earlier linear analysis, Fig. 10 from the nonlinear analysis shows no symmetry of the cost about the line of zero separation angle. In fact, there are many cases where the results deviate from the linear analysis dramatically. For example, refer to Fig. 10, and consider the case where $\theta_2 = 100$ deg, $\theta_4 = -100$ deg, and $t_f = 1$. In this case, the total cost for $s_1$ to rendezvous with $s_2$ is 10.475, whereas the total cost to rendezvous with $s_4$ is only 1.869. It is not always true, however, that a rendezvous with $s_2$ always costs more than a rendezvous with $s_4$. For a smaller time $t_f = 0.75$ with the same separation angles $\theta_2$ and $\theta_4$, it is found that the cost for $s_1$ to rendezvous with $s_2$ is 1.881, but the cost for $s_1$ to rendezvous with $s_4$ is 4.041.

### Initial and Terminal Coastings

The preceding analysis did not consider any initial or final coastings. To this end, let $f(\tau)$ denote the coefficient of $|\theta_2|$ in Eq. (15), that is,

$$f(\tau) = \frac{\sqrt{5 - 8\cos\tau + 3\cos^2\tau}}{|8 - 3\tau\sin\tau - 8\cos\tau|} \quad (16)$$

It can be shown that (as a function of the transfer time $\tau$) $f(\tau)$ possesses similar characteristics with the $\Delta V$ vs $t_f$ curve in Fig. 12. Therefore, the optimal terminal coasting can be calculated the same way as for the nonlinear case. Furthermore, the optimal terminal coasting period is the same for all cases with the same time of flight $t_f$, regardless of the separation angle. This is because the transfer time and the separation angle are decoupled in Eq. (15).

The analysis using the nonlinear equations suggests a different scenario. As seen in Fig. 10, the local minima corresponding to two distinct separation angles occur at different transfer times. Figures 10 and 12 show that a terminal coasting may dramatically

**Table 1 Comparison between the rendezvous costs of satellite 1 with satellites 2 and 4**

| | | | Coasting allowed | | | |
|---|---|---|---|---|---|---|
| | Coasting not allowed | | Rendezvous 2 | | Rendezvous 4 | |
| $t_f$ | Rendezvous 2 | Rendezvous 4 | Coasting time | Cost | Coasting time | Cost |
| 1.0 | 10.475 | 1.869 | 0.25 | 1.881 | N/A | 1.869 |
| 0.75 | 1.881 | 4.041 | N/A | 1.881 | N/A | 4.041 |
| 2.0 | 3.313 | 1.116 | 0.36 | 0.684 | 0.72 | 0.914 |
| 3.5 | 0.625 | 0.694 | 0.78 | 0.428 | 0.21 | 0.358 |

decrease the rendezvous cost for some cases. Let us revisit the case where $t_f = 1$, $\theta_2 = 100$ deg, and $\theta_4 = -100$ deg. Without permitting terminal coasting, a rendezvous with $s_2$ results in a $\Delta V = 10.475$, and a rendezvous with $s_4$ results in a $\Delta V = 1.869$. However, with a terminal coasting of $t_{fc} = 0.25$, the amount of $\Delta V$ for a rendezvous with $s_2$ decreases to 1.881; this is very close to 1.869, the $\Delta V$ required to rendezvous with $s_4$, which cannot be decreased by allowing terminal coasting.

There is still no clear trend whether a rendezvous with $s_2$ or a rendezvous with $s_4$ costs less. Thus far, we have shown that for the case when $\theta_2 = 100$ deg, $\theta_4 = -100$ deg, and $t_f = 0.75$ a rendezvous with $s_4$ costs more than a rendezvous with $s_2$. None of these two costs can be decreased by allowing terminal coasting. If $t_f = 2$, however, and without terminal coasting, a rendezvous with $s_2$ requires $\Delta V = 3.313$, and a rendezvous with $s_4$ requires $\Delta V = 1.116$. For both cases, the cost can be decreased by a final coasting. From Fig. 10, the coasting periods for a rendezvous with $s_2$ and $s_4$ can be calculated as $t_{fc} = 0.36$ and $t_{fc} = 0.72$, respectively. As a result of these terminal coastings, a rendezvous with $s_2$ requires $\Delta V = 0.684$, which is less than the cost for a rendezvous with $s_4$ (which in this case decreases to $\Delta V = 0.914$ due to coasting). However, if the total time of travel is $t_f = 3.5$, then, and without a terminal coasting, a rendezvous with $s_2$ costs 0.625 and a rendezvous with $s_4$ costs 0.694. Introducing a terminal coasting of $t_{fc} = 0.78$ decreases the cost of $s_2$ to $\Delta V = 0.428$. This is more than the cost required to rendezvous with $s_4$, which is $\Delta V = 0.358$ with a terminal coasting of $t_{fc} = 0.21$. These results are summarized in Table 1.

**Rendezvous with Two Preceding Satellites**

We now turn our attention to the following question, also arising from the scenario depicted in Fig. 13. For the sake of simplicity, we assume that $\theta_3 \leq 180$ deg. Given a transfer time $t_f$, the objective is to determine the best rendezvous scenario for $s_1$, that is, whether a rendezvous with $s_2$ or a rendezvous with $s_3$ will require a smaller $\Delta V$. The intuitive answer is that a rendezvous with $s_2$ is better because $s_3$ is farther away from $s_1$ than $s_2$ and, hence, it costs more. This is again consistent with Eq. (15) from the linear analysis. However, as is shown next, this intuition from the linear analysis is not always correct. To see this, let us consider the case when $t_f = 1.85$. It is clear from Fig. 10 that the cost monotonically increases with the initial separation angle in the interval $\theta_0 \in [0, 180]$ deg. That is, for this particular $t_f$, it costs more for $s_1$ to rendezvous with $s_3$ than to rendezvous with $s_2$. However, for the case when $t_f = 1.28$, the cost monotonically increases with $\theta_0$ in the interval $\theta_0 \in [0, 19.192]$ deg and decreases monotonically in the interval $[19.192, 180]$ deg. That is, when $\theta_2 \geq 19.192$ deg and $t_f = 1.28$, the cost for $s_1$ to rendezvous with $s_3$ is always less than the cost for $s_1$ to rendezvous with $s_2$.

The preceding observations do not consider any terminal coasting. With terminal coasting permitted, it is seen that in most cases, and for the same time of travel, the larger the separation angle the larger the cost. However, it is not difficult to find cases where rendezvous with a satellite farther away costs less than with one close by. For example, let us consider the case when $t_f = 1.42$. For separation angles $\theta_0 < 115$ deg, we can see from Fig. 10 that the cost monotonically increases with $\theta_0$ if terminal coasting is permitted. However, when $\theta_0 > 115$ deg and if terminal coasting is permitted, the cost monotonically decreases with $\theta_0$ (although terminal coasting here does not help decrease the cost). This observation is again inconsistent with the results from the linear analysis.

The discrepancy between the linear and nonlinear analysis suggests limitations of the applicability of the classical linear C–W equations when used in rendezvous problems. The C–W equations are based on the assumption that the orbit of the target vehicle and the transfer orbit of the chaser vehicle are not far apart from a reference circular orbit (in the order of several kilometers radially). In addition, due to the presence of secular terms in the solutions to the C–W equations,[11] these equations are more suitable for transfers with short time span. Despite these shortcomings, the C–W equations have found success in many proximity rendezvous and docking applications. However, as shown in this study, caution has to be exercised when applying the C–W equations to general rendezvous problems, even when both the chaser and the target vehicles are in the same circular orbit. This is because in most rendezvous scenarios the resulting transfer orbits are ellipses, which do not necessarily stay in the vicinity of the circular orbit.

**Conclusions**

We have studied the minimum-$\Delta V$, fixed-time, two-impulse rendezvous problem between two spacecraft moving along two coplanar circular orbits in the same direction. A fixed-time transfer problem between two points fixed on the two orbits is solved using the solution of the multiple-revolution Lambert problem. A solution procedure that involves the introduction of an auxiliary transfer problem is found, which greatly facilitates the calculations. The characteristics of the auxiliary transfer problem are thoroughly explored and are used to narrow down the $2N_{\max} + 1$ solution candidates for the optimal fixed-time fixed-endpoint transfer problem to at most two. When this procedure is used, the cost of the original moving-target rendezvous problem without initial and terminal coasting is obtained for all cases with different separation angles and times of travel. A contour plot of the cost is obtained as a function of the separation angle and the transfer time. This contour plot along with a sliding rule helps one find the optimal initial and terminal coasting periods and, thus, yields solutions to the original rendezvous problem. It is found that, for moving-target rendezvous problems with both the chaser and target vehicles in the same circular orbit, the reliance on the contour plot to calculate the optimal transfer orbit is eliminated. For problems where the chaser and target are in different circular orbits, the contour plot is needed only for rendezvous scenarios that cannot be achieved by the Hohmann transfer. Several examples demonstrate our procedure. These examples also show that a linear analysis may lead to erroneous conclusions.

**Appendix: Derivation of d$\Delta V$/d$a$**

In this Appendix, we give the derivation of d$\Delta V$/d$a$ that can be used to determine $a_{\min}$. The expression for $\Delta V$ is given in Eqs. (3) and (4). The velocities at $P_1$ and $P_2$ on the transfer orbit are given by[9]

$$v_1 = \sqrt{2(\mathcal{E} + \mu/r_1)}, \qquad v_2 = \sqrt{2(\mathcal{E} + \mu/r_2)} \qquad (A1)$$

where $\mathcal{E} = -\mu/(2a)$ is the energy of the transfer orbit. The elevation angles $\phi_1$ and $\phi_2$ are given by

$$\phi_1 = \tan^{-1} \frac{e \sin f_1}{1 + e \cos f_1}, \qquad \phi_2 = \tan^{-1} \frac{e \sin f_1}{1 + e \cos f_1}$$

where $e$ is the eccentricity of the transfer orbit and $f_1$ and $f_2$ are the true anomalies at $P_1$ and $P_2$ on the transfer orbit, which are given in the following equations:

$$e = \left[ 1 - \frac{4(s - r_1)(s - r_2)}{d^2} \sin^2 \left[ \frac{\alpha + \beta}{2} \right] \right]^{\frac{1}{2}} \qquad (A2)$$

$$f_1 = \cos^{-1} \left[ \frac{1}{e} \left( \frac{p}{r_1} - 1 \right) \right] = \cos^{-1} \left[ \frac{a(1 - e^2) - r_1}{e r_1} \right] \qquad (A3)$$

$$f_2 = \cos^{-1} \left[ \frac{1}{e} \left( \frac{p}{r_2} - 1 \right) \right] = \cos^{-1} \left[ \frac{a(1 - e^2) - r_2}{e r_2} \right] \qquad (A4)$$

It can be verified that $\Delta V$ is only a function of $a$, provided that $r_1$, $r_2$, and $\theta$ or $d$ are given. Thus, the derivative of $\Delta V$ with respect to $a$ is given by

$$\frac{\mathrm{d}\Delta V}{\mathrm{d}a} = \frac{\mathrm{d}\Delta V_1}{\mathrm{d}a} + \frac{\mathrm{d}\Delta V_2}{\mathrm{d}a} \qquad (A5)$$

From Eq. (4), we have

$$\frac{\mathrm{d}\Delta V_1}{\mathrm{d}a} = \frac{\partial \Delta V_1}{\partial v_1}\frac{\mathrm{d}v_1}{\mathrm{d}a} + \frac{\partial \Delta V_1}{\partial \phi_1}\frac{\mathrm{d}\phi_1}{\mathrm{d}a}$$

where

$$\frac{\partial \Delta V_1}{\partial v_1} = \frac{2v_1 - 2v_{1c}\cos\phi_1}{2\sqrt{v_1^2 + v_{1c}^2 - 2v_1 v_{1c}\cos\phi_1}} = \frac{v_1 - v_{1c}\cos\phi_1}{\Delta V_1}$$

$$\frac{\mathrm{d}v_1}{\mathrm{d}a} = \frac{\partial v_1}{\partial \mathcal{E}}\frac{\mathrm{d}\mathcal{E}}{\mathrm{d}a} = \frac{1}{2}\frac{2}{v_1}\left[-\frac{\mu}{2}\left(-\frac{1}{a^2}\right)\right] = \frac{\mu}{2a^2 v_1}$$

$$\frac{\partial \Delta V_1}{\partial \phi_1} = \frac{2v_1 v_{1c}\sin\phi_1}{2\sqrt{v_1^2 + v_{1c}^2 - 2v_1 v_{1c}\cos\phi_1}} = \frac{v_1 v_{1c}\sin\phi_1}{\Delta V_1}$$

and $\mathrm{d}\phi_1/\mathrm{d}a$ can be obtained as follows:

$$\frac{\mathrm{d}\phi_1}{\mathrm{d}a} = \frac{\partial \phi_1}{\partial f_1}\frac{\mathrm{d}f_1}{\mathrm{d}a} + \frac{\partial \phi_1}{\partial e}\frac{\mathrm{d}e}{\mathrm{d}a} \qquad (A6)$$

In Eq. (A6),

$$\frac{\partial \phi_1}{\partial f_1} = \left\{1\bigg/\left[1 + \left(\frac{e\sin f_1}{1 + e\cos f_1}\right)^2\right]\right\}$$

$$\times \frac{e\cos f_1(1 + e\cos f_1) - e\sin f_1(-e\sin f_1)}{(1 + e\cos f_1)^2}$$

$$= \frac{e\cos f_1 + e^2}{1 + 2e\cos f_1 + e^2}$$

$$\frac{\partial \phi_1}{\partial e} = \left\{1\bigg/\left[1 + \left(\frac{e\sin f_1}{1 + e\cos f_1}\right)^2\right]\right\}$$

$$\times \frac{\sin f_1(1 + e\cos f_1) - e\sin f_1\cos f_1}{(1 + e\cos f_1)^2}$$

$$= \frac{\sin f_1}{1 + 2e\cos f_1 + e^2}$$

and $\mathrm{d}f_1/\mathrm{d}a$ can be obtained from Eq. (A3) as follows:

$$\frac{\mathrm{d}f_1}{\mathrm{d}a} = \frac{\partial f_1}{\partial e}\frac{\mathrm{d}e}{\mathrm{d}a} + \frac{\partial f_1}{\partial a}$$

where

$$\frac{\partial f_1}{\partial e} = -\left\{1\bigg/\sqrt{1 - \left[\frac{a(1 - e^2) - r_1}{er_1}\right]^2}\right\}$$

$$\times \frac{-2ae^2 r_1 - [a(1 - e^2) - r_1]r_1}{e^2 r_1^2}$$

$$= \frac{ae^2 + a - r_1}{e\sqrt{(er_1)^2 - [a(1 - e^2) - r_1]^2}}$$

$$\frac{\partial f_1}{\partial a} = \frac{e^2 - 1}{\sqrt{(er_1)^2 - [a(1 - e^2) - r_1]^2}}$$

and

$$\frac{\mathrm{d}e}{\mathrm{d}a} = \frac{\partial e}{\partial(\alpha + \beta)}\frac{\mathrm{d}(\alpha + \beta)}{\mathrm{d}a} \qquad (A7)$$

In Eq. (A7)

$$\frac{\partial e}{\partial(\alpha + \beta)} = -\frac{(s - r_1)(s - r_2)\sin(\alpha + \beta)}{ed^2}$$

and it is derived in Ref. 5 that

$$\frac{\mathrm{d}(\alpha + \beta)}{\mathrm{d}a} = -\frac{1}{a}\left(\tan\frac{\alpha}{2} + \tan\frac{\beta}{2}\right)$$

The expression for $\mathrm{d}\Delta V_2/\mathrm{d}a$ can be obtained similarly.

## Acknowledgment

## References

[1] Sparks, A., "Satellite Formationkeeping Control in the Presence of Gravity Perturbations," *Proceedings of the American Control Conference*, IEEE Publications, Piscataway, NJ, 2000, pp. 844–848.

[2] Wang, P. K., Hadaegh, F. Y., and Lau, K., "Synchronized Formation Rotation and Attitude Control of Multiple Free-Flying Spacecraft," *Journal of Guidance, Control, and Dynamics*, Vol. 22, No. 1, 1999, pp. 28–35.

[3] Alfriend, K. T., and Schaub, H., "Dynamics and Control of Spacecraft Formations: Challenges and Some Solutions," *Advances in the Astronautical Sciences*, Vol. 106, Univelt, Inc., San Diego, CA, 2000, pp. 205–223.

[4] Helton, M. R., "Refurbishable Satellites for Low Cost Communications Systems," *Space Communication and Broadcasting*, Vol. 6, June 1989, pp. 379–385.

[5] Prussing, J. E., "A Class of Optimal Two-Impulse Rendezvous Using Multiple-Revolution Lambert Solutions," *Advances in the Astronautical Sciences*, Vol. 106, Univelt, Inc., San Diego, CA, 2000, pp. 17–39.

[6] Lion, P. M., and Handelsman, M., "Primer Vector on Fixed-Time Impulsive Trajectories," *AIAA Journal*, Vol. 6, No. 1, 1968, pp. 127–132.

[7] Battin, R. H., *An Introduction to the Mathematics and Methods of Astrodynamics*, AIAA Education Series, AIAA, Reston, VA, 1999, pp. 237–342.

[8] Prussing, J. E., "Geometrical Interpretation of the Angles $\alpha$ and $\beta$ in Lambert's Problem," *Journal of Guidance Control, and Dynamics*, Vol. 2, No. 5, 1979, pp. 442, 443.

[9] Hale, F. J., *Introduction to Space Flight*, Prentice–Hall, Englewood Cliffs, NJ, 1994, pp. 24–50.

[10] Clohessy, W. H., and Wiltshire, R. S., "Terminal Guidance System for Satellite Rendezvous," *Journal of Aerospace Sciences*, Vol. 27, Sept. 1960, pp. 653–658.

[11] Prussing, J. E., and Conway, B. A., *Orbital Mechanics*, Oxford Univ. Press, Oxford, England, U.K., 1993, pp. 99–154.